1995

Lattice- and Molecular-Dynamics Studies of $RbLiSO_4$

V. Katkanant
California State University, Fresno, California

John R. Hardy
University of Nebraska - Lincoln

Physical Review B 51, 137 - 145 (1995)

Lattice- and molecular-dynamics studies of $RbLiSO_4$

V. Katkanant
Department of Physics, California State University, Fresno, California 93740-0037

J. R. Hardy
Department of Physics and Center for Electro-Optics, University of Nebraska-Lincoln, Nebraska 68588-0111

Abstract

Using our previously developed method for calculating parameter-free potential-energy surfaces for ionic molecular crystals, specifically sulfates, we study phase transitions in $RbLiSO_4$ by means of lattice and molecular dynamics. We found that the high-temperature phase I (*Pnam*) is highly unstable and transforms to the observed lower temperature phase VI ($P112_1/n$) at about 475–525 K. Compared with isomorphous $CsLiSO_4$, there are more branches of unstable modes in the *Pnam* phase for $RbLiSO_4$. The maximum instability of these modes occurs away from the zone center, $q=(0.118a^*,0,0)$, which implies that a high-order incommensurate phase could form during the phase transformation. The driving mechanism of these phase transitions is directly related to the rotational ordering of tetrahedral SO_4^{2-} groups. The rms values of the deviations of the S-O bonds from their orientations in the *Pnam* phase to those in the $P112_1/n$ phase were found to be approximately ±23–25°.

URL: http://link.aps.org/doi/10.1103/PhysRevB.51.137

DOI: 10.1103/PhysRevB.51.137

Lattice- and molecular-dynamics studies of $RbLiSO_4$

V. Katkanant
Department of Physics, California State University, Fresno, California 93740-0037

J. R. Hardy
Department of Physics and Center for Electro-Optics, University of Nebraska-Lincoln, Nebraska 68588-0111
(Received 7 March 1994)

Using our previously developed method for calculating parameter-free potential-energy surfaces for ionic molecular crystals, specifically sulfates, we study phase transitions in $RbLiSO_4$ by means of lattice and molecular dynamics. We found that the high-temperature phase I (*Pnam*) is highly unstable and transforms to the observed lower temperature phase VI ($P112_1/n$) at about 475–525 K. Compared with isomorphous $CsLiSO_4$, there are more branches of unstable modes in the *Pnam* phase for $RbLiSO_4$. The maximum instability of these modes occurs away from the zone center, $\mathbf{q}=(0.118\mathbf{a}^*,0,0)$, which implies that a high-order incommensurate phase could form during the phase transformation. The driving mechanism of these phase transitions is directly related to the rotational ordering of tetrahedral SO_4^{2-} groups. The rms values of the deviations of the S-O bonds from their orientations in the *Pnam* phase to those in the $P112_1/n$ phase were found to be approximately $\pm 23-25°$.

I. INTRODUCTION

In our recent paper[1] we reported the results of an *a priori* study of the statics and dynamics of the double-sulfate $CsLiSO_4$. Our basic finding was that the major structural reconstruction in this system was driven by an inherent "double well" in the lattice potential energy surface for the sulfate rotation. Specifically, the major such instability is against rotations about the *Pnam* **a** axis. In the cesium based compound, this instability produces only one clear phase transition below 300 K, although the transition takes place over an appreciable temperature range ($\sim$40 K). We were also able to identify the probable origin of this diffuseness as very weak intersulfate coupling along the **a** axis, which manifests itself both as a very flat dispersion curve (<1 cm^{-1} dispersion along the entire [100] axis) and in a tendency for our molecular dynamics to "freeze in" probably spurious superlattice structure along the **a** axis. In the vicinity of the basic *Pnam*-$P112_1/n$ transitions, if the intersulfate coupling along **a** is weak, a superlattice structure, having higher entropy, is preferred. In the simulation, it persists down to 0 K because the enhanced lattice strain energy present in the real system is very poorly represented in the molecular-dynamics supercell.

Isomorphous $RbLiSO_4$ (RLS), by contrast with $CsLiSO_4$ (CLS), has a complex phase diagram showing no fewer than six phases within a 37-K range, between 438–474.5 K.[2] A great many experimental measurements have been made on this compound, including x-ray[2,3] and neutron diffractions,[4] differential scanning calorimetry,[5] dielectric measurements,[6] infrared spectroscopy,[7] and microscopic studies,[8] etc. RLS undergoes incommensurate-commensurate phase transitions and has disordered, antiferroelectric, ferroelectric and paraelectric phases. Moreover, an electric field can induce another polar phase[2] with the modulation wave vector $k=\frac{1}{3}\mathbf{a}_0^*$ where $a_0^*=2\pi/a_0$ and a_0 is the basic cell dimension in the high-temperature structure above 475 K. In this high-temperature phase, RLS is disordered and belongs to orthorhombic space group *Pnam* (D_{2h}^{16}) with four formula units per unit cell. It transforms through several successive phases to a monoclinic paraelectric phase below 438 K having the $P112_1/n(C_{2h}^5)$ space group. This has the same number of atoms in the unit cell as the high-temperature *Pnam* phase. However, the modulation period is $2a_0$ in the antiferroelectric phase (IV) and is elongated to $5a_0$ in the ferroectric phase (VI). The most surprising fact, given that these phases are clearly variants on the basic transition in CLS, is that these transition temperatures are $\sim 2.5-3$ times higher than the 160–200 K transition in the CLS. Since our work on the latter compound has not revealed any major inadequacy in our treatment of the pair potentials involving Li^+, the one area not previously studied and most suspect, our approach should be capable of reproducing this major difference between the Rb^+, and Cs^+ based compounds. Nevertheless, we do not expect to be able to reproduce the complex sequence of transitions if there is again very weak intersulfate coupling along the **a** axis. Furthermore, our simulation has to employ the usual periodic boundary conditions, which thus will not allow us to achieve the incommensurate structure.

II. *AB INITIO* POTENTIAL-ENERGY SURFACE AND STATIC RELAXATION

The procedure followed was essentially the same as that employed for CLS.[1] Once again pair potentials external to the SO_4^{2-} group are derived using the Gordon-Kim technique from the ionic charge densities. Those involving members of the SO_4^{2-} group are generat-

ed from the spherically averaged decomposition of the charge density of the sulfate group, obtained using the quantum chemistry GAUSSIAN package.[9] Motion internal to these units is handled by the harmonic force field generated by that code. The calculated optimized structures gave near-perfect tetrahedra with average S-O bond lengths of 1.474 Å *(Pnam)* and 1.444 Å $(P112_1/n)+$ compared to the experimental values[2] of 1.433 Å and 1.445 Å for the high- and low-temperature structures, respectively.

We determined the static equilibrium configurations of both *Pnam* and $P112_1/n$ structures by static relaxation, first imposing the appropriate symmetry constraints and then without any such symmetry constraints. In Figs. 1 and 2, the resultant structures are shown, while in Tables I and II: the associated structural parameters are listed, together with their experimental counterparts. The statically relaxed structure of the low-temperature phase, obtained subject to the $P112_1/n$ symmetry constraints, and that found without imposing any constraints were essentially the same and are dynamically stable. The theoretical structure strongly resembles the experimental structure as can be seen in Fig. 2. For RLS, unlike CLS, the agreement between theory and experiment for the *Pnam*

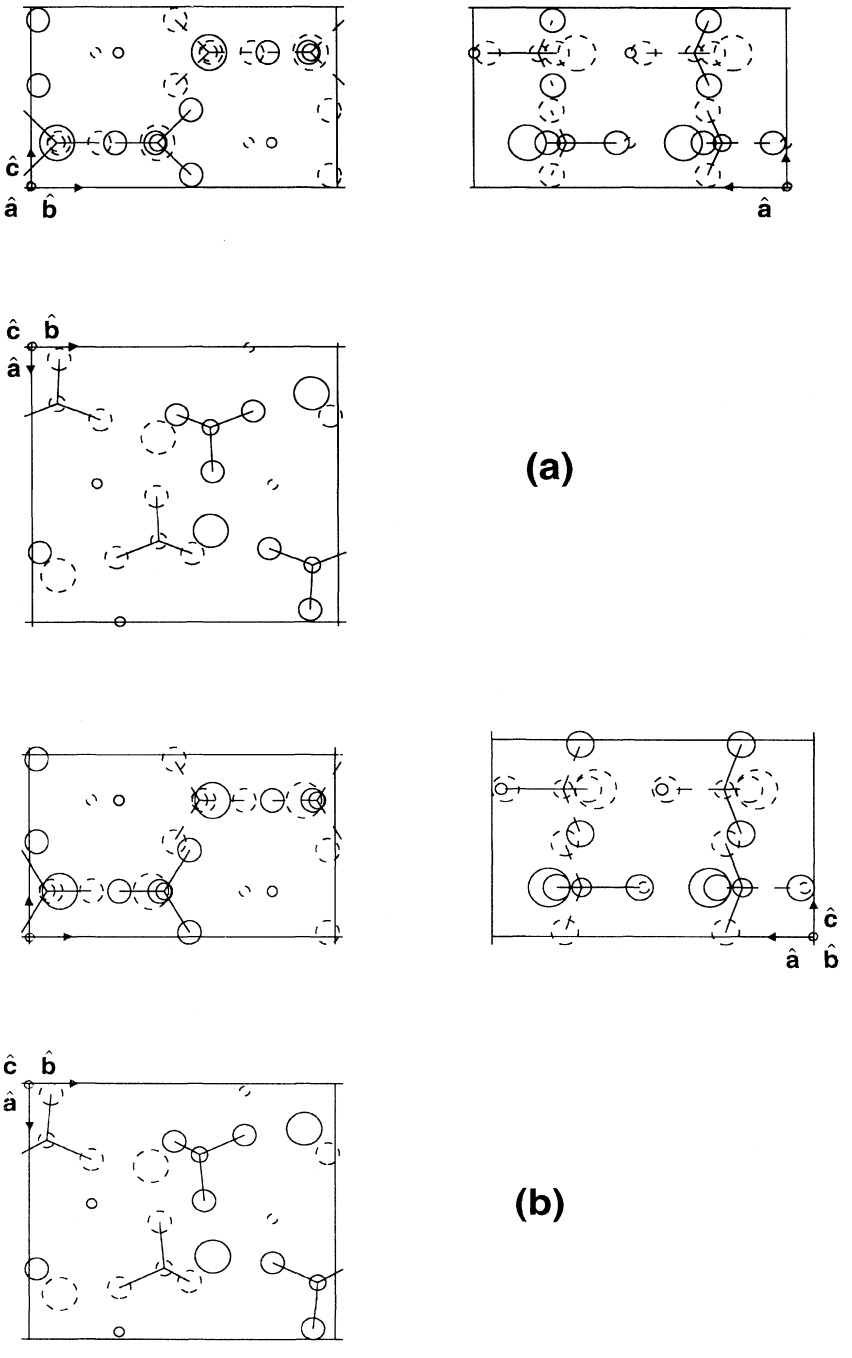

FIG. 1. Projection of the (a) experimental and (b) theoretical static structure of $RbLiSO_4$ in the *Pnam* phase. A lattice vector pointing out of the page is represented by a circle. The smallest circles represent the Rb atoms and the largest circles represent Li atoms. Bonds (straight lines) connect each S and the nearest four O atoms. Broken lines denote ions lying above or below the plane.

phase is not as good, but is within the magnitude of the thermal parameters. Kunishige and Mashiyama[2] have pointed out that the large thermal parameters of the oxygen atoms in these compounds may indicate disorder of the sulfate tetrahedra.

Surprisingly, the general relaxation of the theoretical high-temperature *Pnam* phase achieved a stable *polar* structure as shown in Fig. 3. This polar structure is consistent with the fact that it is one of the two equally probable forms of the disordered high-temperature phase reported in Ref. 2. In this reference, the crystal structure analysis and Fourier maps show double peaks around the positions of O(1) and O(3). The final atomic positions for this disordered structure were obtained by averaging the coordinates of these two equally probable sites; these averages we used as our initial input parameters and to compare with our results in our theoretical calculations. These two configurations of the SO_4^{2-} tetrahedron can be reached by rotations of about $\pm 23°$ from the mirror plane about an axis nearly parallel to the *a* axis. This polar

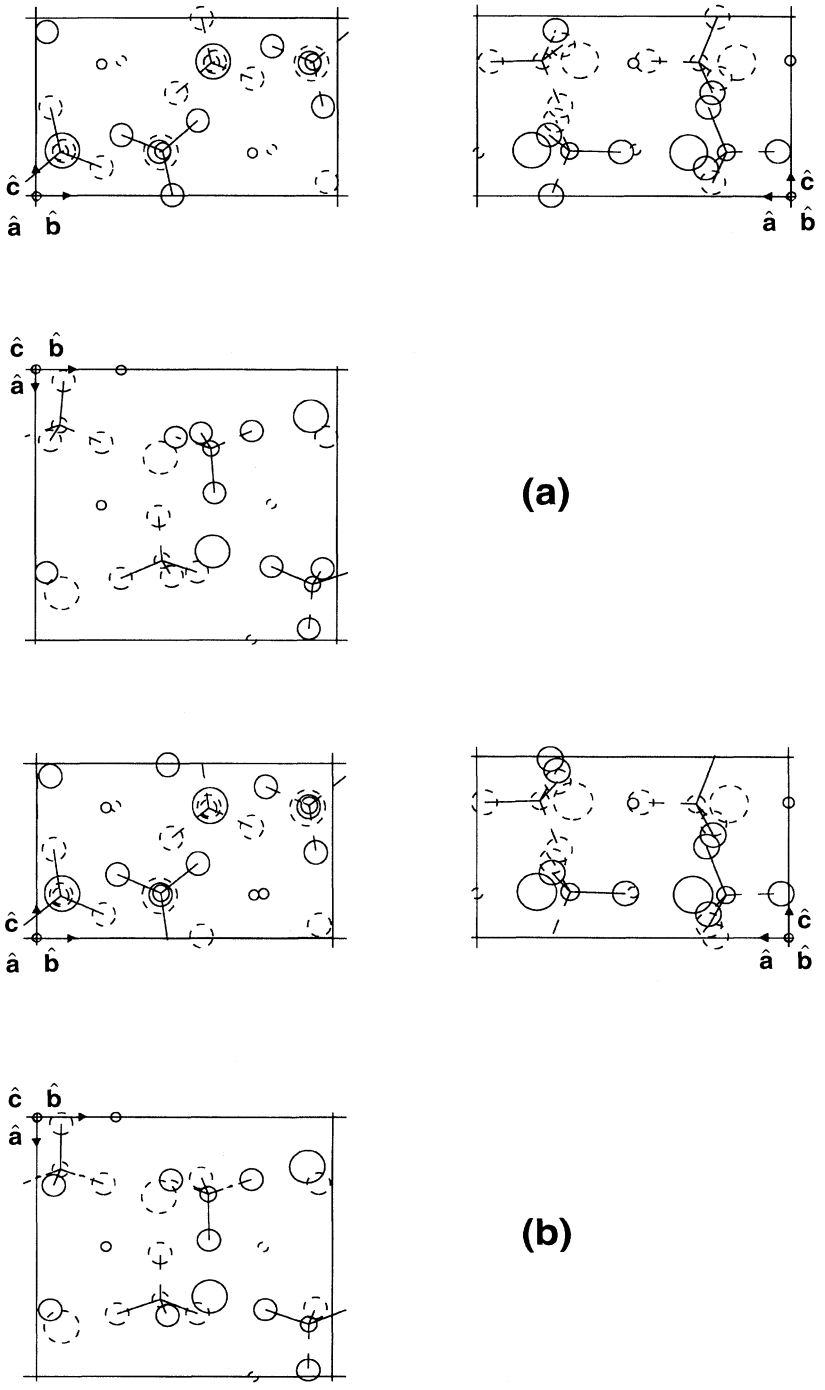

FIG. 2. Projection of the (a) experimental and (b) theoretical static structure of $RbLiSO_4$ in the $P112_1/n$ phase.

TABLE I. Experimental (Ref. 1) and theoretical structural parameters for the *Pnam* phase of $RbLiSO_4$. (The lattice constants are given in angstroms.)

Parameters	Experiment	Theory	% Diff.	Diff.
a	8.701	8.121	7	0.58
b	9.174	9.038	1	0.14
c	5.304	5.284	0	0.02
x/a of S(1)	0.2064	0.2215	−7	−0.13
y/b of S(1)	0.0848	0.0576	32	0.25
x/a of Rb(1)	0.5020	0.5287	−5	−0.23
y/b of Rb(1)	0.2129	0.2051	4	0.07
x/a of Li(1)	0.3301	0.3234	2	0.06
y/b of Li(1)	0.4148	0.3992	4	0.14
x/a of O(1)	0.2659	0.2989	−12	−0.29
y/b of O(1)	0.2244	0.2045	9	0.18
x/a of O(2)	0.0444	0.0412	7	0.03
y/b of O(2)	0.0915	0.0724	21	0.18
x/a of O(3)	0.2527	0.2741	−8	−0.19
y/b of O(3)	−0.0248	−0.0249	0	0.00
z/c of O(3)	0.0696	0.0236	66	0.24

structure is one of the other double-well potential energy surfaces in both our static and dynamic calculations and will be discussed fully in the next section.

The minimum energies for the high- and low-temperature structures are −22.0072 and −22.1931 eV/formula unit, respectively, while the energy for the polar structure is −22.1903 eV/formula unit. These

TABLE II. Experimental (Ref. 1) and theoretical structural parameters for the $P112_1/n$ low-temperature phase of $RbLiSO_4$. (The lattice constants are given in angstroms.)

Parameters	Experiment	Theory	% Diff.	Diff.
a	8.717	8.296	5	0.42
b	9.134	8.773	4	0.36
c	5.303	5.112	4	0.19
Angle	89°54′	89°51′		
x/a of S(1)	0.2064	0.2024	2	0.03
y/b of S(1)	0.0808	0.0793	2	0.01
z/c of S(1)	0.2473	0.2432	2	0.02
x/a of Rb(1)	0.5030	0.5004	1	0.02
y/b of Rb(1)	0.2177	0.2337	−7	−0.15
z/c of Rb(1)	0.7405	0.7452	−1	−0.02
x/a of Li(1)	0.3268	0.3084	6	0.16
y/b of Li(1)	0.4131	0.4140	0	−0.01
z/c of Li(1)	0.2449	0.2427	1	0.01
x/a of O(1)	0.0425	0.0250	41	0.15
y/b of O(1)	0.0928	0.0818	12	0.10
z/c of O(1)	0.2523	0.2513	0	0.01
x/a of O(2)	0.2718	0.2598	4	0.10
y/b of O(2)	0.2176	0.2257	−4	−0.07
z/c of O(2)	0.1587	0.1359	14	0.12
x/a of O(3)	0.2644	0.2647	0	0.00
y/b of O(3)	0.0481	0.0559	−16	−0.07
z/c of O(3)	0.4975	0.5107	−3	−0.07
x/a of O(4)	0.2493	0.2565	−3	−0.06
y/b of O(4)	−0.0355	−0.0463	1	0.10
z/c of O(4)	0.0776	0.0733	6	0.02

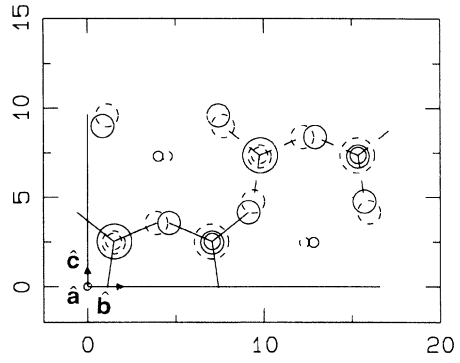

FIG. 3. Relaxed polar structure obtained by unrestricted static relaxation from the *Pnam* structure. Note the difference in phase between adjacent SO_4^{2-} groups compared with the $P112_1/n$ structure in Fig. 2.

findings hint at a significant difference in the phase diagrams of these two compounds. This could clearly relate to the fact that the RLS forms polar ferroelectric structures at both 473.1 and 457 K,[2] intermediate between *Pnam* and $P112_1/n$ phases, whereas CLS shows no ferroelectric behavior whatsoever.

Finally, we would like to mention that these crystal structures have a pseudohexagonal cell[8] with the ratio of $b/c \cong 1.732$ or $\sqrt{3}$. Experimentally, for CLS this value is 1.733 and 1.729 for the *Pnam* and $P112_1/n$ phases, which are closer to 1.732 than those of the RLS which are 1.730 and 1.722. Our static relaxed structures gave b/c ratios for the RLS as 1.716 and 1.711 and for the CLS as 1.738 and 1.723 for the *Pnam* and $P112_1/n$ phases, respectively. Clearly, RLS is less hexagonal and the fit to experiment marginally worse.

III. LATTICE-DYNAMICAL STUDIES OF $RbLiSO_4$ STRUCTURES

We then computed the dispersion curves for both relaxed structures, and in Fig. 4 we show only those for the [100] direction since there are apparently no new instabilities along the **b** and **c** directions. Again the *Pnam* phase is actually unstable; more so than for CLS. There are four negative branches, which represent imaginary frequencies, along all three directions, [100], [010], and [001]. Moreover, the absolute maximum instability lies not at the zone center, but at $\mathbf{q}=(0.118\mathbf{a}^*,0,0)$ indicating a preference for a high-order incommensurate phase, in qualitative agreement with the experimental behavior. As in the case of CLS, the negative branches of dispersion curves are very flat and extend over the whole zone, indicating weak multiple instabilities. However, the lattice-dynamical calculation for the polar structure shows absolutely no unstable modes which indicates that it has reached a metastable configurations. The $P112_1/n$ structure is apparently stable down to 0 K, but at $T\sim450$ K it may still be possible for an incommensurate modulated phase to be preferred since thermal disorder

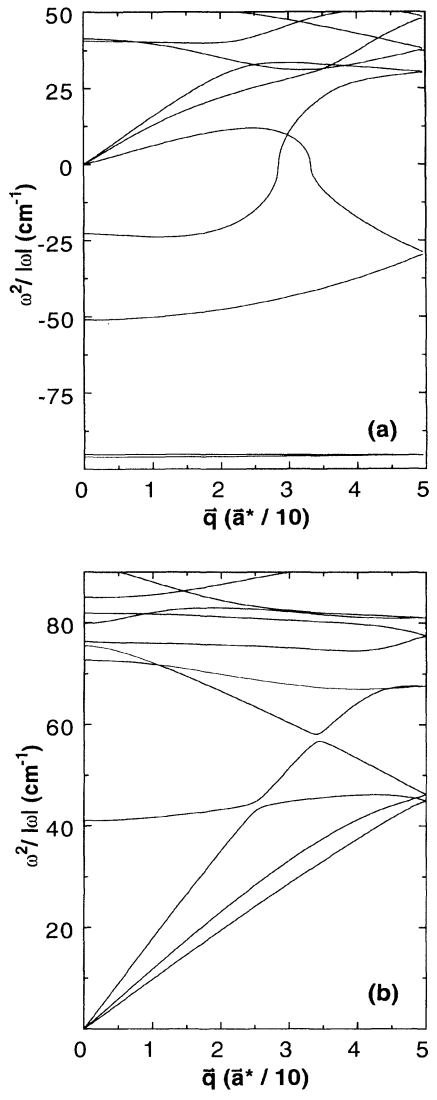

FIG. 4. Dispersion curves along the [100] direction for the theoretical (a) *Pnam* and (b) $P112_1/n$ structures.

will certainly sample the almost degenerate ferroelectric configuration.

IV. MOLECULAR-DYNAMIC SIMULATIONS OF THE PHASE TRANSITIONS

We performed constant- or zero-pressure algorithm molecular-dynamics (MD) calculations[10] to simulate and follow the real time movement of a collection of interacting atoms. To provide an infinite-size lattice for the simulation, we imposed periodic boundary conditions. This was the only restriction that applied to the supercell since all of the ion positions and all of the lattice vectors were allowed to change during the simulation. The time increment between two successive steps was chosen to be 0.002 ps, which is small enough to integrate accurately the equations of motion for a system containing such a light atom as Li. In order to determine thermal mean values for velocities, positions, etc., the corresponding instantaneous values were averaged over several different time intervals of increasing length. Specifically, we employed 12, 24, 42, and occasionally 80 ps averaging to test for genuine thermalization. When the average is unchanged by doubling the time, then thermalization has been achieved. We found that the 42 ps scan is long enough for a $2\mathbf{a}\times 2\mathbf{b}\times 2\mathbf{c}$ supercell to meet our goal of elucidating the phase transitions in RLS.

Initially, we performed molecular-dynamics calculations to simulate and examine directly the lower-temperature phase structure starting from the high-temperature relaxed *Pnam* structure. We quenched a unit cell with 28 ions by gradually reducing the total kinetic energy of the sample in stages to zero, in order to reach the ground state. We hoped to reproduce realistically the experimentally observed monoclinic $P112_1/n$ structure at low temperature, as in the case of CLS. However, as we mentioned in the preceding section, experimentally this compound passes through two different ferroectric phases before it settles into the $P112_1/n$ ground state. Therefore, it is likely that our simulation could freeze into one of the polar structures, as was found in our static studies (Fig. 3). The other possible polar structure which the unit cell reached after we repeated this molecular-dynamics relaxation several times is shown in Fig. 5. The potential energies of both these structures are exactly equal at 183.30 meV per formula unit below that of the theoretical *Pnam* structure and are 0.21 meV higher than $P112_1/n$ structure. This degeneracy occurs because the two structures correspond to switched polarities. Thus in RLS, the *Pnam* structure is higher in energy than the $P112_1/n$ phase by 183.51 meV. Whereas the energy different between the *Pnam* and $P112_1/n$ structures in the CLS compounds is 45.2 meV and the polar structure is higher than the $P112_1/n$ by about 0.78 meV. It is evident that the excess energy of the polar phase over the $P112_1/n$ ground state, when compared to the *Pnam*-$P112_1/n$ energy difference, is at least an order of magnitude smaller in RLS compared with CLS (Table III illustrates this situation). It is thus

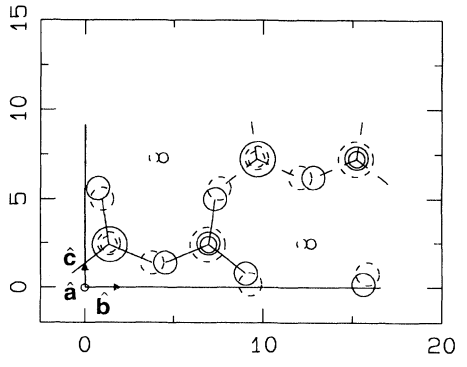

FIG. 5. One of the polar structure obtained by MD relaxation: This is identical in energy to the polar structure in Fig. 3 and simply corresponds to the state of reversed polarity.

TABLE III. Comparison of the relative energies of the three phases of (a) $RbLiSO_4$ and (b) $CsLiSO_4$.

(a) $RbLiSO_4$	eV/formula unit
Pnam	-22.0072
183.30 meV, 183.51 meV	
Polar	-22.1903
0.21 meV, $P11_21/n$	-22.1931

(b) $CsLiSO_4$	eV/formula unit
Pnam	-21.8581
44.42 meV, 45.2 meV	
Polar	-21.9025
0.78 meV, $P11_21/n$	-21.9033

not surprising that our theoretical studies show that RLS has a strong tendency to lock-in to the polar structure as compared with CLS. Also, the CLS simulations show only weak spontaneous polarization ($\mathbf{P}_c$) fluctuations on heating through T_c while RLS shows very strong $\mathbf{P}_c$ fluctuations over about 120±20 K range as the temperature is increased through T_c. Thus, in RLS polar and nonpolar states clearly compete and the system is "frustrated." Consequently, a complex series of phase transitions is likely to appear in RLS, which is consistent with the experimental phase diagram.

In view of the presence of two very flat branches in the dispersion curves (Fig. 4) for *Pnam* phase, resembling the situation in CLS, we adopted a similar procedure to determine T_c for the *Pnam-P11*$2_1/n$ instability. Thus we set up first an $\mathbf{a}\times\mathbf{b}\times\mathbf{c}$ $P11_2_1/n$ lattice and monitored the $\mathbf{b}\cdot\mathbf{c}$ angle (α) as the order parameter. It should be noted that α can be both less than or greater than 90°: the latter possibility occurs when the monoclinic phase forms with its obtuse angle at the origin. We then repeated this procedure for a $2\mathbf{a}\times\mathbf{b}\times\mathbf{c}$ cell. Finally, we studied a $5\mathbf{a}\times\mathbf{b}\times\mathbf{c}$ cell. Our purpose in using two-fold and five-fold cells along the **a** direction is to allow all possible distortions, i.e., SO_4^{2-} rotations and ionic displacements, etc., consistent with the observed antiferroelectric and ferroelectric structures with the modulation wave vectors $\mathbf{k}=\frac{1}{2}\mathbf{a}_0^*$ and $\mathbf{k}=\frac{2}{5}\mathbf{a}_0^*$, respectively. In Fig. 6, we show the order parameter connected with a gradual rotation of the sulfate tetrahedron with temperature for those runs. Clearly, the single cell is too small, leading to a transition which is too abrupt. The cell doubled along **a** is better showing a more gradual transition, while the $5\mathbf{a}\times\mathbf{b}\times\mathbf{c}$ supercell shows additional stages. However, to see this last behavior clearly it is necessary to monitor the SO_4^{2-} rotations, since the narrowness of the supercell exaggerates the change in α angle induced by SO_4^{2-} rotations, and gives the impression that the transition is essentially complete when only one or two SO_4^{2-} units have switched. In reality, all five cells only become free at essentially the same temperature where the $\mathbf{b}\cdot\mathbf{c}$ angle curves in Fig. 6(a) intersect the 90° axis; i.e., in all cases $T_c \cong 450$–470 K, in close agreement with the experimental T_c value for the first *Pnam* instability (474.5 K). The fluctuations of the spontaneous polarizations along **c**

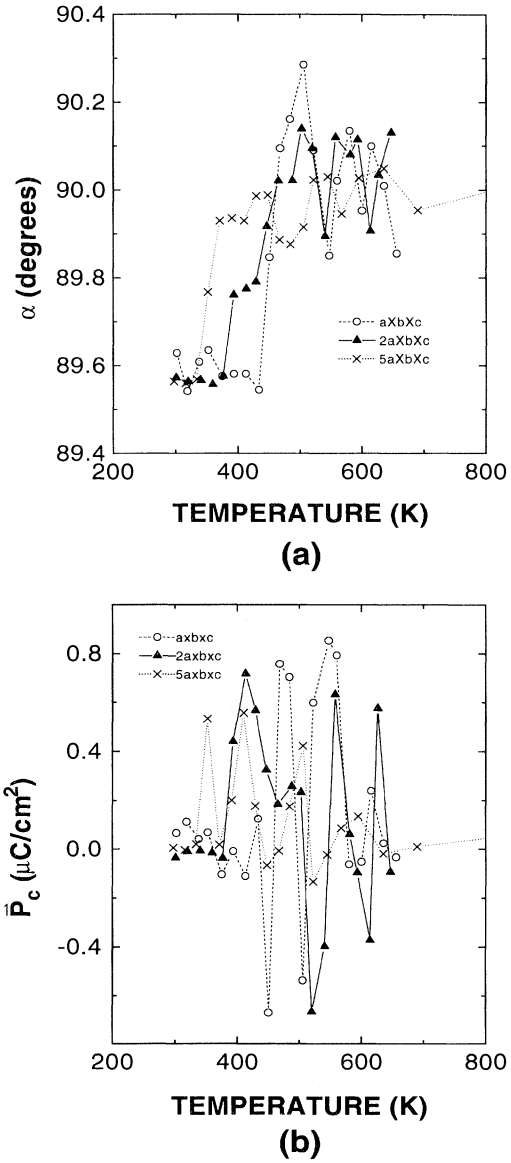

FIG. 6. (a) The order parameter α (the angle between the lattice vectors **b** and **c** as functions of temperature for three different supercell dimensions, obtained from molecular-dynamics heating runs, (b) Polarization versus temperature for the same three supercells.

($\mathbf{P}_c$), are also shown in Fig. 6(b).

However, as was mentioned above, the narrowness of the supercell may not reproduce closely enough the real system for our purpose. Also, we wished to be consistent with our work on the CLS, thus we then doubled our supercell size along **b** and **c** to **a**×2**b**×2**c** (112 ions) and used an averaging time of 24 ps. In the present case, we limited the cell size not to be multiplied along **a**, owing to our finding for the CLS that the system tends to assume that higher periodicity at the cost of marginally (10 K/formula unit for the polar state) higher static energy. This is consistent with the very flat unstable branches of the dispersion curves along **a**. The resultant order parameter (angle a) for both cooling and heating runs are plotted as a function of temperature in Fig. 7. Apparently, in both cases the structure transforms over sensibly the same temperature range, about 500±20 K. However, for the cooling run the system "locked-in" to the negative polar state ($-\mathbf{P}_c$), hence $\alpha=90°$. This was not the case for the CLS simulation, which only showed the polar state during transformation to the low-temperature $P112_1/n$ structure if the unit cell was multiplied along **a**. As a consequence of this, we would argue that our MD simulation agrees qualitatively with the experimental observation of a complex sequence of phase transformations for the RLS. This is another indication of the reliability of our potentials.

To obtain better statistics and investigate further, we increased our supercell size to 2**a**×2**b**×2**c** (224 ions) and extended the averaging time to 36, 42, and 80 ps, to ensure true thermal equilibrium. Again the order parameter and polarization versus temperatures of the cooling run and two heating runs of 42 and 80 ps, respectively, are compared in Fig. 8. It is clearly apparent that the onset of the transition lies in the range 500–550 K, which corresponds closely to that above which the orthorhombic high-temperature structure is stable. Figure 9 shows the MD simulation of high- and low-temperature structure of 2**a**×2**b**×2**c** at 600 and 300 K, respectively.

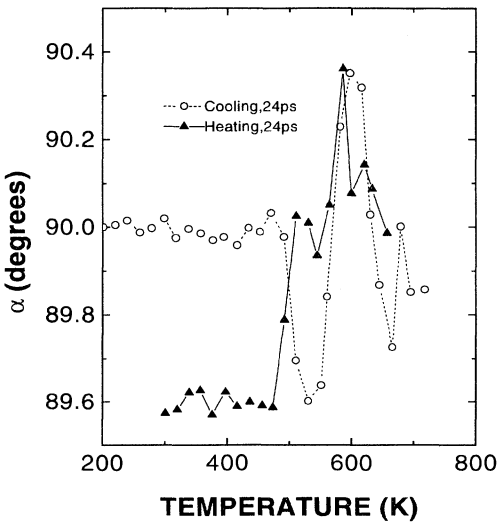

FIG. 7. The order parameter α versus temperature for both cooling and heating scans of **a**×2**b**×2**c** with an averaging time of 24 ps.

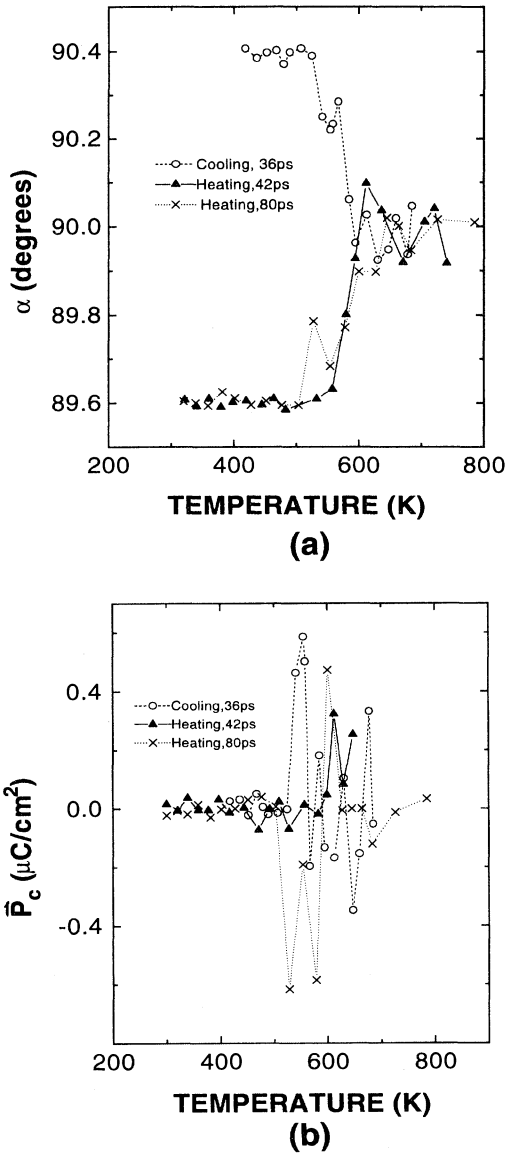

FIG. 8. (a) The order parameter α and (b) the polarization versus temperatures for cooling and heating scans of 2**a**×2**b**×2**c** with averaging over successively longer times: 36, 42, and 80 ps.

V. DISCUSSION

On the basis of the results described above, it would appear that our procedure for constructing parameter-free interionic potentials for ionic molecular solids, has proved itself to be as reliable for RLS as for CLS. In both cases, we face the problem of superlattice formation in our simulations, which we feel may arise mainly from the enhanced role of elastic energy in the true free energy

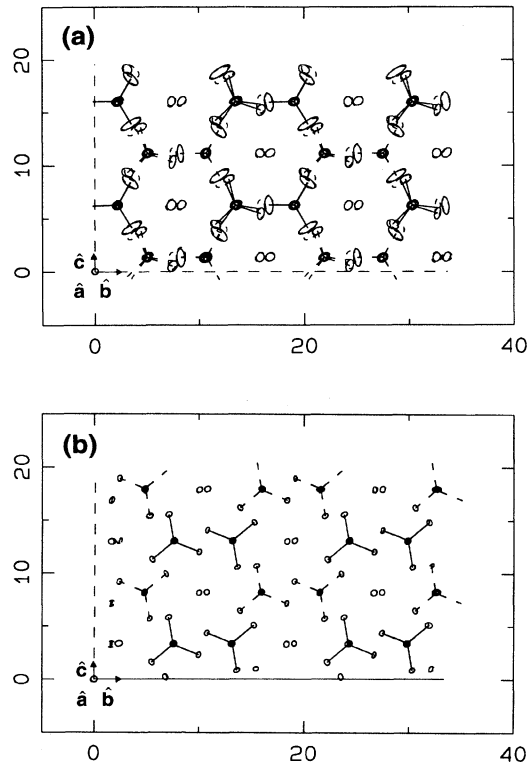

FIG. 9. bc cross sections of the MD average structures of $RbLiSO_4$ at (a) ~600 K and (b) ~300 K.

of these systems. In both cases, this appears to have its origin in the much weaker intersulfate coupling along the a axis, which causes the simulations to favor maximum multiplicity of SO_4^{2-} orientations about that axis. However, in all cases this is achieved at the cost of enhanced elastic energy, primarily in the form of b·c angle shear reduction. Since this gain is ~2–10 K/formula unit, it is only for supercells large enough for this, in total, to be $\sim k_B T_c$ (where k_B is the Boltzman constant) that it can begin to affect the phase diagram in a realistic manner. However, for a true equilibrium regime to the attained in such large systems, impractically long averaging and equilibration times would be required.

While we have focused on comparison between the experimental and theoretical phase transitions and associated T_c values, we have also predicted the large number of structural parameters not defined by symmetry (see Tables I and II) and these agree with experiments, apart from the lattice constants, to within the cited errors. Not only is this gratifying, given that the potentials are entirely parameter-free, but it also implies that we have the capability of *predicting* the properties of compounds involving these ions, in situations which may be difficult to access experimentally. One example is the stress dependence of the Raman spectrum at megabar stresses. Another related possibility is to that of examining the phase diagram at the comparable (or higher) stresses ambient in the earth's mantle.

It is also useful to examine our results within the general context of structural instabilities. In the first place, these double alkali sulfates are only one of the very many types of ionic molecular solids in which the molecular ions are completely isolated, in the sense that they unconnected by shared corner ions, thus the interionic coupling is very weak (one can see this in the very small differences in energy between the ferroelastic and ferroelectric ground states, which differ basically in the rotation patterns of adjacent SO_4^{2-} ions, and also in the very flat phonon dispersion curves). Hence, the rotational double wells for the SO_4^{2-} ions are *local* and it is the depths of these which determine T_c: well below this temperature the ions would rotate, whether or not there is *any* intersulfate coupling. However, one would not then expect any long-range order and, to achieve ordering in these systems, one requires long-range correlated motion over a sufficient number of unit cells such that the energy difference between, for example, ferroelectric and ferroelastic phases, is $\sim k_B T_c$. Hence the limitations of molecular dynamics with its inherent "trade off" between supercell size and length of averaging time.

This also has an important general implication: if one deliberately "spoils" long-range correlations in ionic molecular solids by introducing disorder, then the system may never achieve *long-range* static order, but rather below T_g ($\sim T_c$) will form a "glassy" phase as has been observed in e.g., CKN, $Ca_{0.4}K_{0.6}(NO_3)_{1.4}$.[11]

It is also useful to characterize the basic double well that drives the rotational instability. If θ is the rotational angle, then the simplest double-well form is

$$U(\theta) = -a\theta^2 + b\theta^4 \text{ , where } a,b>0 \text{ ,} \tag{1}$$

which has a minimum at

$$\theta_0 = \sqrt{a/2b} \tag{2}$$

and

$$U(\theta_0) = \frac{-a^2}{4b} = \frac{-a}{2}\theta_0^2 \tag{3}$$

for RLS $\theta_0^1 = 25°$ and for CLS $\theta_0^2 = 13°$. Therefore,

$$\frac{U(\theta_0^1)}{U(\theta_0^2)} \cong 4 \tag{4}$$

if a is approximately constant. From Table III, the actual value of this is $183.51/45.2 = 4.06$. Clearly these are sufficiently close to indicate that Eq. (1) is an adequate representation of $U(\theta)$.

However, there is another consequence of this ratio that is disturbing. On any reasonable basis, one expects $k_B T_c \sim (\text{const}) \times (\theta_0)^2$. This implies that T_c(RLS) $\sim 4T_c$(CLS): in reality, the ratio ≅2:1. This suggests that the intersulfate coupling constant also changes substantially between compounds.

In our previous calculations for CLS, we settled on using a a×2b×2c supercell to provide us the best measure of the T_c associated with the basic rotational instability of the sulfate groups. For this cell, we obtained a single well-defined transition in both heating and cooling with

only minor ($\sim 5\%$) hysteresis. We found a theoretical T_c value of 200–250 K which is in satisfactory agreement with the experimental value ~ 200 K. However, for $RbLiSO_4$ while the heating run showed a clear transition at 475–525 K, the cooling run, while transforming over substantially the same temperature range, did so into an orthorhombic state which was polar and is produced by counterclockwise rotation of the SO_4^{2-} pairs in the unit cell (see Figs. 3 and 5). Moreover, the heating run shows clear evidence of a transient (~ 120 K) polar phase during the transition. This polar structure was also encountered during CLS studies, but only for supercells multiplied along **a** and only during the cooling runs. Static relaxation to this state revealed it to have an energy of about 10 K/formula unit higher than the ground state. A similar calculation for CLS revealed a comparable energy difference, however, proportionately, this is at least an order of magnitude larger, relative to T_c, than for RLS, particularly when one recognizes that lattice expansion on heating of RLS to ~ 600 K is likely to reduce significantly this already very small difference in static energy. As a consequence, there is in RLS a temperature range over which the basic ferroelectric and nonferroelectric instabilities compete, resulting in the complex sequence of phases observed experimentally, which appear to be composed of *ferroelectric* layers with their polarizations alternating between adjacent *Pnam* unit cells. This is consistent with the fact that only the odd multiplicity phases show a net polarization, while the cell doubled phase is identified as *antiferroelectric*. Our simulations, restricted in size as they have to be, can only reveal the *signature* of this behavior from the nonpolar to polar unit cells, i.e., the transient polar phase. Conversely, the fact that no such transition is observed in our CLS simulations indicates that for this compound there is no such competition. Consequently the phase diagram is simple with one single transition from the ground state to the *Pnam* phase.

Finally, we would like to conclude that RLS and CLS belong to tridymite related structure, the same as NH_4LiSO_4. The characteristic features of these pseudohexagonal structures are a framework consisting of six-membered rings of alternating SO_4^{2-} and LiO_4 tetrahedra normal to the **a** axis.[12] The basal plane of the tetrahedron is nearly parallel to the **bc** plane, and the cations lie approximately at the centers of the large cavities in the tetrahedral framework. Empirically it appears that the different phases of these compounds are strongly related to the possible orientations of the SO_4^{2-} tetrahedra. Additionally, the tetrahedra are rotated around **a** in order to obtain a better coordination with the cations. The smaller the cation the larger the tetrahedral rotation and hence the higher the temperature at which the ordering starts. These empirical observations are clearly in accord with our theoretical calculations: the rotation of the sulfate tetrahedron in RLS is more violent (approximately $\pm 25°$ about **a** axis) in going from *Pnam* to $P112_1/n$, and *vice versa*, as against $\pm 13°$ in CLS.

Guided by comparison of the ranges of existence of the disordered phases of RLS ($T > 475$ K) and CLS ($T > 202$ K), with the size (radius) of the cations, $R^+_{Rb} = 1.48$ Å and $R^+_{Cs} = 169$ Å. Pietraszko,[13] by means of x ray and optical studied, revealed that the substitution of Rb by Cs resulted in an increase of the stability range of the disordered phase and in a reduction of the number of possible phases. It will be the aim of our future theoretical work to extend our insight into the mechanism of the phase transitions of these two compounds by study of mixed RLS and CLS systems.

ACKNOWLEDGMENTS

The work of V.K. was supported by the Research Corporation. The work of J. R. Hardy was supported by the Army Research Office.

[1]V. Katkanant, H. M. Lu, and J. R. Hardy, Phys. Rev. B **46**, 5982 (1992).

[2]Atsuhiro Kunishige and Hiroyuki Mashiyama, J. Phys. Soc. Jpn. **56**, 3189 (1987).

[3]Hiroyuki Mashiyama, Katsuhiko Hasebe, Sigetosi Tanisaki, Yoshihiro Shiroishi, and Shozo Sawada, J. Phys. Soc. Jpn. **47**, 1198 (1979); W. Steurer, H. Wittman, and H. Jagodzinski, Acta Cryst. **B42**, 11 (1986).

[4]F. Frey, H. Jagodzinski, A. Pietraszko, and C. Zeyen, Solid State Commun. **46**, 557 (1983).

[5]Yoshihiro Shiroishi and Shozo Sawada, J. Phys. Soc. Jpn. **46**, 148 (1979); **40**, 911 (1976).

[6]Hiroyuki Mashiyama and H. G. Unruh, J. Phys. Soc. Jpn. **54**, 822 (1985).

[7]Vijay Varma, Ramendu Bhattacharjee, J. R. Fernandes, and C. N. R. Rao, Solid State Commun. **76**, 627 (1990).

[8]A. I. Kruglik, S. V. Misyul, and M. A. Simonov, Kristallografiya **24**, 582 (1979) [Sov. Phys. Crystallogr. **24**(3), 333 (1979)]; Sigetosi Tanisaki *et al.* Acta Cryst. **B36**, 3084 (1980).

[9]H. M. Lu and J. R. Hardy, Phys. Rev. Lett. **64**, 661 (1990), Phys. Rev. B **42**, 8339 (1990), and the references cited there.

[10]M. Parrinello and A. Rahman, Phys. Rev. Lett. **45**, 1196 (1980).

[11]G. Li, W. M. Du, X. K. Chen, H. Z. Cummins, and N. J. Tao, Phys. Rev. A **45**, 3867 (1992).

[12]W. A. Dollase, Acta Cryst. **B25**, 2298 (1969).

[13]A. Pietraszko, Acta Cryst. **A37**, C109 (1981).